

Electronic Supplementary Information

Na⁺ diffusion mechanism and transition metal substitution in tunnel-type manganese-based oxides for Na-ion rechargeable batteries

Irene Quinzeni, Kotaro Fujii, Marcella Bini, Masatomo Yashima and Cristina Tealdi

Table SI-1 – Pair potential parameters used to describe the Na_{0.44}MnO₂ system (cut-off 20 Å).

<i>interaction</i>	<i>A (eV)</i>	<i>ρ (Å)</i>	<i>C (eV Å⁶)</i>	<i>Spring constant, K (eV Å⁻²)</i>	<i>Shell charge, Y (e)</i>
Na··O	997.11	0.342619	0.00	-	0.00
Mn··O	1267.50	0.3193	0.00	-	0.00
Cu··O	3860.60	0.2427	0.00	999999	1.00
O··O	22764.30	0.1490	43.00	42	-2.24

$$U_{ij} = \frac{q_i q_j}{r} + A_{ij} \exp\left(-\frac{r_{ij}}{\rho_{ij}}\right) - \frac{C_{ij}}{r_{ij}^6}$$

Buckingham function:

Table SI-2 – Lists of models prepared for the MD simulations.

<i>label</i>	<i>composition</i>	<i>percentage occupancy of the Na ions in the 1D channel</i>
modA	Na _{0.44} MnO ₂	60%
modB	Na _{0.44} MnO ₂	71%
modC	Na _{0.44} MnO ₂	90%
Cu10-modA	Na _{0.49} Mn _{0.9} Cu _{0.1} O ₂	60%
Cu10-modB	Na _{0.49} Mn _{0.9} Cu _{0.1} O ₂	71%
Cu10-modC	Na _{0.49} Mn _{0.9} Cu _{0.1} O ₂	90%
Cu10-modA-el	Na _{0.44} Mn _{0.9} Cu _{0.1} O ₂	60%
Cu10-modB-el	Na _{0.44} Mn _{0.9} Cu _{0.1} O ₂	71%
Cu10-modC-el	Na _{0.44} Mn _{0.9} Cu _{0.1} O ₂	90%

Table SI-3 – EDS microanalysis results for NMO and NMCO samples.

Sample	Atomic %		
	Na	Mn	Cu
NMO	14.3	31.5	-
NMCO	15.62	27.41	2.36

Table SI-4 – Comparison between experimental (neutron diffraction data, this study) and calculated structural parameters.

<i>Lattice parameters and volume</i>	<i>Experimental</i>	<i>Calculated</i>	<i>Difference %</i>
Lattice volume (\AA^3)	703.34(8)	701.4673	-0.27
a (\AA)	9.241(6)	9.1885	-0.57
b (\AA)	26.660(17)	26.4828	-0.66
c (\AA)	2.8550(18)	2.8827	0.97

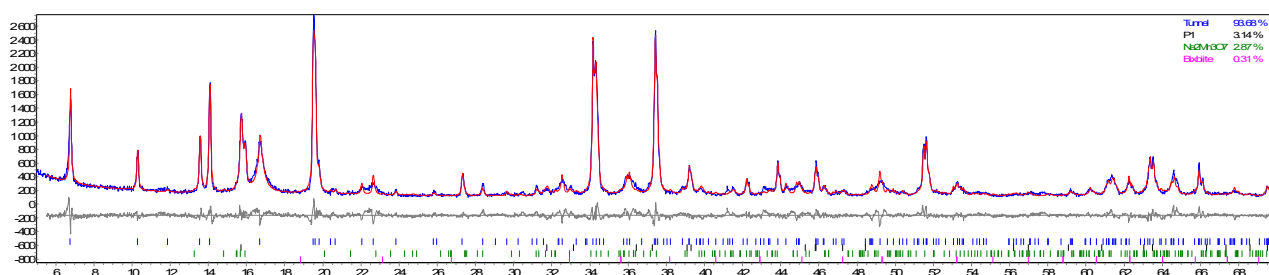


Fig. SI-1. Experimental and calculated (Rietveld refinement) XRD pattern of the NMCO sample. The experimental (blue) and calculated (red) patterns are compared; in the bottom, the difference curve (grey) and the bars of the expected reflections positions of the different phases (tunnel-type NMO, blue; P1 NMO polymorph, black; $\text{Na}_2\text{Mn}_3\text{O}_7$, green and Mn_2O_3 , pink) are also shown.

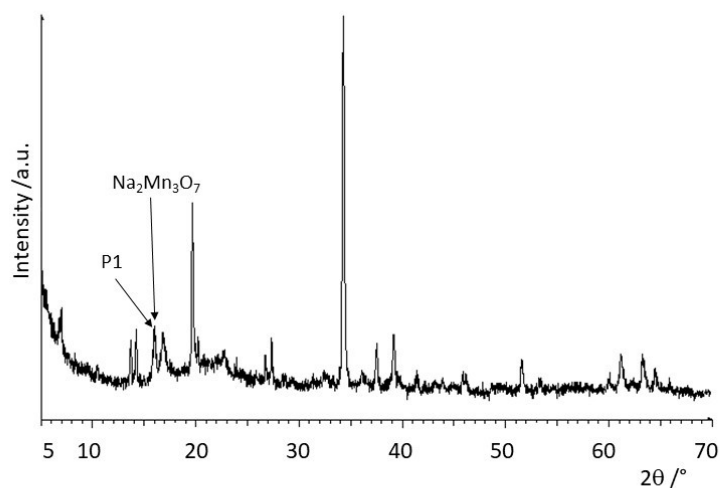


Fig. SI-2. Ex-situ XRD pattern of NMCO after GCPL measurements.

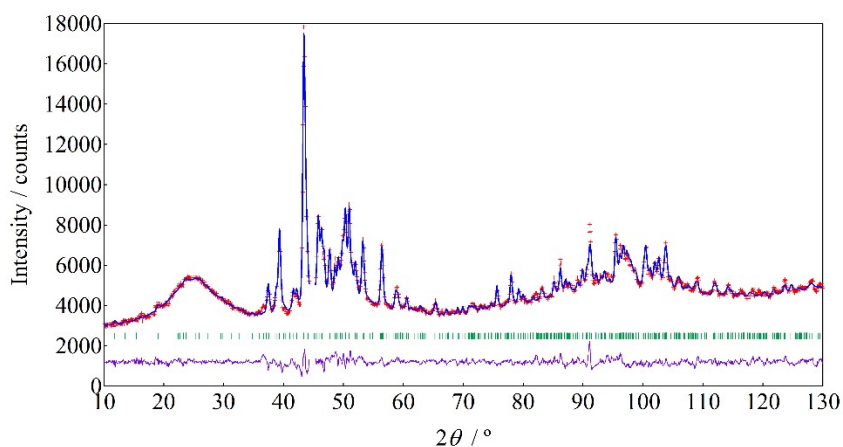
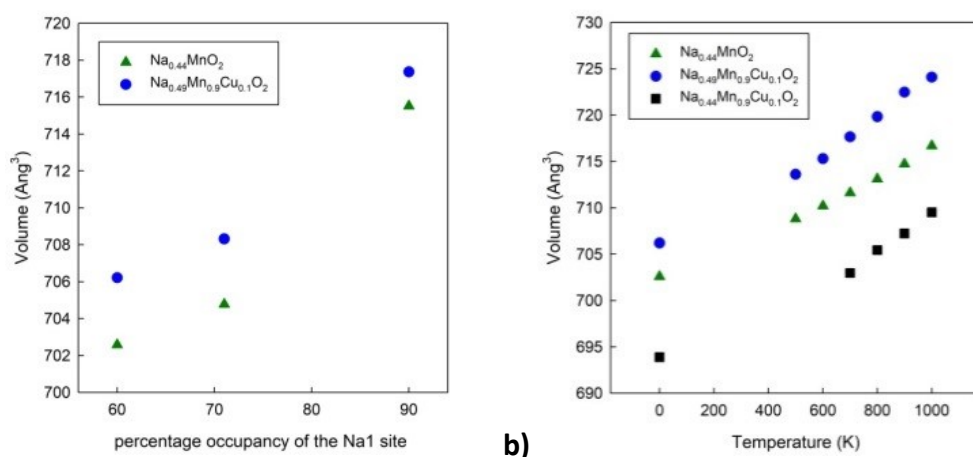


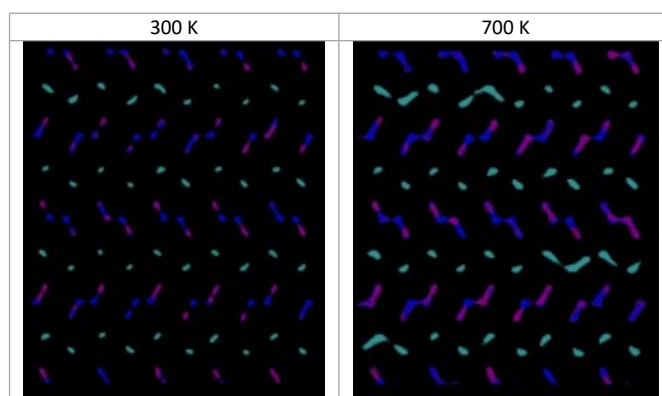
Fig. SI-3. Rietveld patterns of neutron diffraction data NMO at 1073 K. Red crosses, the blue line and the purple line denote the observed, calculated and difference plots, respectively. Green tick marks stand for the calculated peak positions.



a)

b)

Figure SI-4. Cell volume trend a) as a function of the percentage of occupation of the Na1 site for two different compositions; b) as a function of temperature for three different models and 60% occupation on the Na1 site.



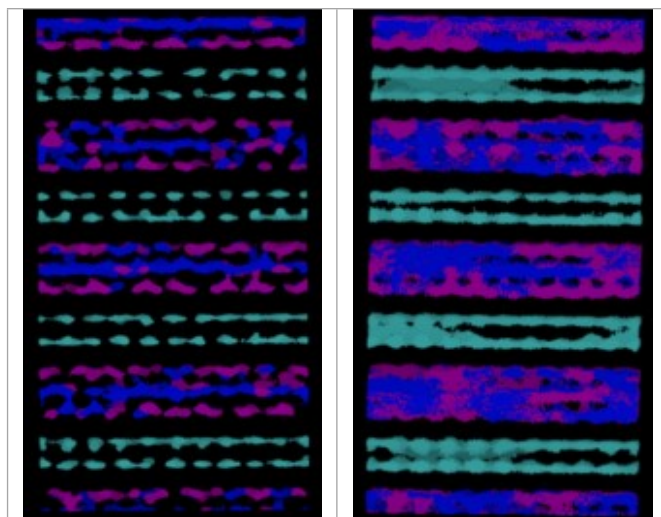


Figure SI-5. Comparison among the Na⁺ ion trajectories of a sample of Na_{0.44}MnO₂ composition, with 71% of Na1 sites occupied, as the temperature changes: view along the c axis (upper panel); view along the a axis (lower panel). For the sake of clarity, only the positions occupied by the Na⁺ ions are reported; each point represents a position occupied by Na⁺ along the simulation time. Legend: Na1 - cyan; Na2 - purple; Na3 – blue.